THE JOURNAL OF PHYSICAL CHEMISTRY B

Article

pubs.acs.org/JPCB

Multistage Unfolding of an SH3 Domain: An Initial Urea-Filled Dry Molten Globule Precedes a Wet Molten Globule with Non-Native Structure

Amrita Dasgupta,[†] Jayant B. Udgaonkar,*[,†] and Payel Das*[,‡]

[†]National Centre for Biological Sciences, Tata Institute of Fundamental Research, Bangalore 560065, India

[‡]Computational Biology Center, IBM Thomas J. Watson Research Center, 1101 Kitchawan Road, Yorktown Heights, New York 10598, United States

Supporting Information

ABSTRACT: The unfolding of the SH3 domain of the PI3 kinase in aqueous urea has been studied using a synergistic experiment−simulation approach. The experimental observation of a transient wet molten globule intermediate, I_U, with an unusual non-native burial of the sole Trp residue, W53, provides the benchmark for the unfolding simulations performed (eight in total, each at least 0.5 μs long). The simulations reveal that the partially unfolded I_U ensemble is preceded by an early native-like molten globule intermediate ensemble I*. In the very initial stage of unfolding, dry globule conformations with the protein core filled with urea instead of water are transiently observed within the I* ensemble. Water penetration into the urea-filled core of dry globule conformations is frequently accompanied by very transient burial of W53. Later during gradual unfolding, W53 is seen to again become transiently buried in the I_U ensemble for a much longer time. In the structurally heterogeneous I_U ensemble, conformational flexibility of the C-terminal β-strands enables W53 burial by the formation of non-native, tertiary contacts with hydrophobic residues, which could serve to protect the protein from aggregation during unfolding.

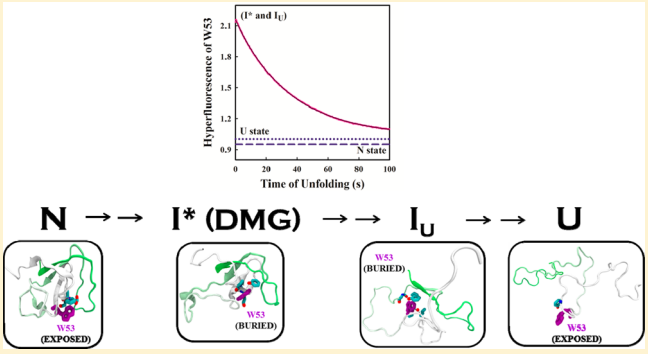

INTRODUCTION

Statistical mechanics theory embodied in the energy landscape approach has provided much insight into the protein folding process.[1−4] Within this framework, simple Gō models have been used extensively to study the folding reactions of small proteins. Such simplified models, which only account for the interactions present in the native state,[5,6] are supported by the observation that the folding rate of a protein is governed by native state topology.[7−10] However, mounting evidence suggests that crucial non-native interactions exist in unfolded states[11,12] as well as in kinetic folding intermediates.[13−19] Those findings have necessitated the development of advanced theoretical models for protein folding, which account for both native and non-native interactions.[20−22] The presence of such non-native interactions might be fundamental to the aggregation of some proteins.[19] Nevertheless, non-native states have also been shown to assist the folding process,[20,23,24] and they may support protein function by aiding conformational switching.[25] It seems that it is the balance between native and non-native interactions[21] which sculpts the free energy landscape of a protein,[7] but the role played by non-native interactions in stabilizing intermediates populated during either folding or unfolding remains to be elucidated in molecular detail for any protein.

SH3 domains have long been used in both simulations and experiments as model proteins for studying the folding and unfolding of small single domain proteins. In particular, the folding and unfolding pathways of the SH3 domain of PI3 kinase (PI3K SH3 domain) have been delineated in detail, in the absence[26−28] and in the presence of cosolutes.[29] A four-state model has been shown to account for both folding and unfolding over the entire range of guanidine hydrochloride (GdnHCl) concentration from 0 to 5 M in the presence of a stabilizing cosolute.[29] An equilibrium and kinetic intermediate (I_U) has been shown to be populated during unfolding in GdnHCl as well as in urea.[26] Importantly, I_U has also been shown to form after the rate-limiting step of folding in native conditions,[26] and hence, structural characterization of I_U provides information about late events during folding. In the native state, the single Trp (W53) residue of the protein is exposed to the solvent (Figure 1a). Recent kinetic studies of the unfolding of PI3K SH3 in GdnHCl have demonstrated that W53 undergoes a transient and partial non-native burial in I_U.[18]

Special Issue: William C. Swope Festschrift

Received: October 8, 2013
Revised: February 25, 2014

   dx.doi.org/10.1021/jp410019f | J. Phys. Chem. B XXXX, XXX, XXX−XXX

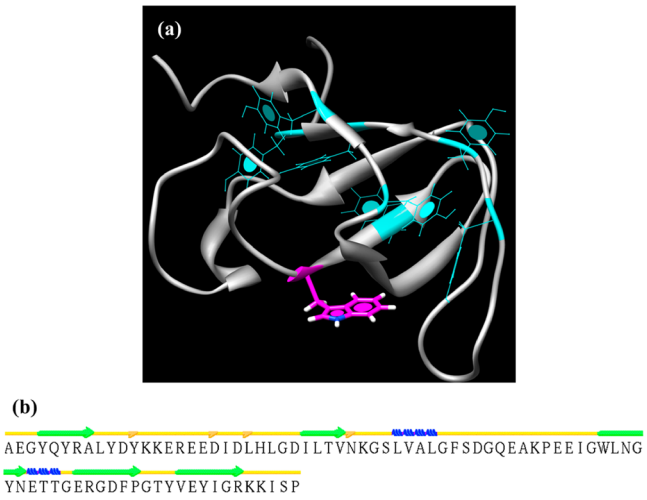

Figure 1. Panel a shows the structure of the PI3K SH3 domain, highlighting the single Trp residue, W53 (magenta), and the seven Tyr residues (cyan) at positions 4, 6, 10, 12, 57, 71, and 74. The ribbon diagram was generated from the PDB file 1PNJ using the UCSF Chimera package from the Resource for Biocomputing, Visualization, and Informatics at the University of California, San Francisco.[77] Panel b shows the assignment of secondary structure to the sequence of the protein using STRIDE.[39] Green arrows indicate β-sheets, blue spirals indicate the 3_{10} helix, and yellow indicates turns or coils.

These findings imply that non-native interactions are present in I_U, but the nature of the specific interactions that drive transient burial of W53 is not yet known.

An important question, not so far addressable by experiment, is whether the unfolding of the PI3K SH3 domain commences with the formation of a dry molten globule (DMG) ensemble in which the tight side chain packing characteristic of the native state hydrophobic core is perturbed without any concomitant penetration of water molecules.[30] Experimental demonstration of the formation of a dry molten globule intermediate has been reported for only a few proteins, and it has become important to determine whether it is a general feature of protein folding and unfolding reactions.[31] Early molecular dynamics (MD) simulations were performed at temperatures probably too high for DMG intermediates to be stable enough to be detected on the unfolding pathway. Only recently have microsecond long MD simulations, carried out to investigate the very early stage of hen egg lysozyme unfolding in aqueous urea at 37 °C, revealed the presence of a transient DMG intermediate.[32] That study showed that the stronger dispersion interaction of urea with the protein, compared to that of water, allows urea to penetrate the protein core earlier than water, resulting in the population of a DMG intermediate. Further simulations showed that it is mainly the hydrophobic residues that remain dry in the DMG, presumably due to their interaction with urea.[33] The generality of urea-filled DMG formation remains, however, to be established. In fact, it has been suggested that the shape and size of the protein may allow water to penetrate first.[34]

In the present study, we employ a combined experiment–simulation approach to obtain a detailed description of the unfolding of the PI3K SH3 domain in aqueous urea. Experimentally, hyperfluorescence is observed in I_U populated during urea-induced unfolding, indicating that W53 has become partially buried and engaged in non-native tertiary interactions in this intermediate. Atomistic molecular dynamics simulations also identify the I_U ensemble with partial burial of W53. The structure of I_U as well as the molecular interactions leading to the non-native burial of W53 is characterized in detail. Interestingly, the simulations also reveal a transient, urea-filled DMG ensemble formed very early during unfolding, the

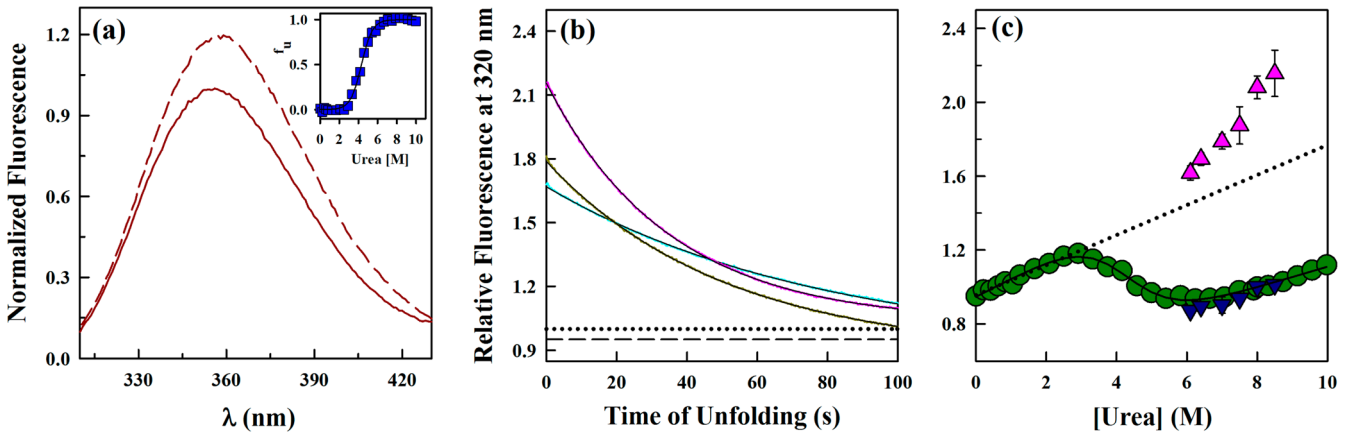

Figure 2. Spectroscopic characterization of urea-induced unfolding of the PI3K SH3 domain at 298 K, pH 7.2. Panel a shows the fluorescence emission spectra with excitation at 295 nm. The solid line in panel a represents the spectrum of the native state in zero denaturant. The dashed line shows the spectrum of the unfolded state in 8 M urea. Each spectrum in panel a was normalized to a value of 1 for the fluorescence signal at 356 nm of the native protein upon excitation at 295 nm. The inset in panel a shows a plot of the fraction of unfolded protein, f_U, versus [urea] determined from measurement of the intrinsic tryptophan fluorescence at 320 nm upon excitation at 295 nm. The continuous line through the data represents a fit to eq 3 which yielded values for the free energy of unfolding and the midpoint of the transition of 4.5 kcal mol^{-1} and 4.3 M, respectively. Panel b shows representative kinetic traces of unfolding at pH 7.2, 298 K. Unfolding in urea was probed by measurement of the change in the intrinsic W53 fluorescence signal at 320 nm with excitation at 295 nm. The data in panel b was obtained when the native protein was diluted into 6 M (cyan), 7 M (dark yellow), and 8 M (pink) urea. Each trace was normalized to a value of 1 for the fluorescence signal of the unfolded protein in 8 M urea (represented by the dashed line). The dotted line represents the signal of the native protein. Panel c shows the equilibrium versus kinetic amplitudes of unfolding monitored using W53 fluorescence at 320 nm upon excitation at 295 nm. (●) equilibrium unfolding transition; (▲) $t = 0$ points; (▼) $t = \infty$ points of the kinetic traces of unfolding. The solid line through the equilibrium points for unfolding in panel c is a fit to eq 1. The dotted line in panel c represents the linearly extrapolated native baseline. The error bars represent the standard deviations from two independent experiments.

dx.doi.org/10.1021/jp410019f | J. Phys. Chem. B XXXX, XXX, XXX–XXX

Table 1[a]

run id	T (K)	length (ns)	highest RMSD (Å)	U visited	DMG visited at (ns)	I_U visited	duration of I_U (ns)	W53 buried in I*	W53 buried in I_U
1	300	758	10.8	no	∼30	yes	80	yes	yes
2	300	584	7.5	no	∼30	yes	543	yes	no
3	300	582	12	no	∼40	yes	140	yes	no
4	310	781	26.3	yes	∼40	yes	99−560	yes	yes
5	310	570	11.6	no	∼50	yes	380	yes	yes
6	400	518	17.3	no	∼8	yes	18−518	yes	yes
7	425	309	29	yes	∼2	yes	8−42	yes	no
8	450	257	28	yes	∼8	yes	13−90	yes	yes

[a]Details of the eight MD runs performed. Five of them were performed at 300−310 K for 500 ns or longer. Three others were performed at higher temperature (400−450 K) to accelerate unfolding kinetics and explore the temperature effect on the unfolding landscape. All simulations were performed in aqueous 8 M urea solution at 1 atm pressure. The population of I_U was determined on the basis of the following criterion: $0.25 \leq Q \leq 0.5$. W53 burial in I_U was found in run 1 (300 K), run 4 (310 K), run 6 (400 K), and run 8 (450 K).

dissolution of which is frequently accompanied by the transient and weak non-native burial of W53. Taken together, these findings highlight the importance of combining experiments and simulations for understanding the underlying molecular picture at different stages of a denaturant-induced protein unfolding reaction.

RESULTS

In this study, experiments characterizing the unfolding of the PI3K SH3 domain in urea have been complemented with long time scale atomistic molecular dynamics simulations of unfolding in urea, to provide molecular insights into the unfolding reaction. The transient non-native burial of W53, which is observed both by experiment and simulation, provides an unfolding benchmark for both studies.

Spectroscopic Characterization and Millisecond Measurements of the Kinetics of the Unfolding of the PI3K SH3 Domain. Figure 2a shows the fluorescence spectra of native (N) protein, and of unfolded (U) protein in 8 M urea, upon excitation of the fluorescence of the sole Trp residue, W53 (Figure 1a), at 295 nm. The spectra clearly indicate that W53 is exposed to the solvent in both the N and U states with emission maxima at 356 nm. This is also depicted in Figure 1a where the structure of the native state shows that W53 is completely exposed to the solvent. The inset in Figure 2a shows that the equilibrium unfolding of the protein (data shown in Figure 2c) in urea using W53 fluorescence at 320 nm can be translated to a plot for fraction unfolded using eq 2, indicating that the N ↔ U transition is two-state-like. Moreover, the data also indicates that, even though W53 is completely exposed in the N and U states, the equilibrium unfolding curve can still be used to monitor a change in the microenvironment of W53 during unfolding in urea. It should be noted that the small increase in the quantum yield of W53 fluorescence upon complete unfolding in urea is not seen for unfolding in GdnHCl.[18]

Figure 2b shows representative kinetic traces of unfolding probed by the measurement of W53 fluorescence at 320 nm. The kinetic traces at >6 M urea do not extrapolate to the value of the fluorescence of the native protein but to fluorescence values exceeding native-state fluorescence. The initial hyperfluorescence of W53 suggests the initial formation of a burst phase intermediate. A comparison of the equilibrium and kinetic amplitudes of the fluorescence-monitored unfolding is shown in Figure 2c. Although the equilibrium unfolding transition of the native state shows the fluorescence to be first increasing, then decreasing, and again increasing, the fluorescence of the $t = 0$ points of unfolding lies significantly above that of the native protein baseline, and increases monotonously. The data in Figure 2c also show that the $t = \infty$ points of the kinetic traces of unfolding lie on the equilibrium unfolding transitions, indicating that all reactions were monitored to completion.

The above results confirm the presence of an unfolding intermediate (I_U) that had been detected before in previous studies using both GdnHCl and urea. In a recent study of the GdnHCl-induced unfolding of the PI3K SH3 domain, transient, non-native partial burial of W53 in this intermediate was observed, which manifested itself as hyperfluorescence of W53 during the kinetics of unfolding.[18] In that study, other possible causes of the transient hyperfluorescence had been considered and discounted.[18] A similar hyperfluorescence is now seen even in urea-induced unfolding of the protein (see above), and thus, it can be concluded that W53 undergoes a transient non-native burial in I_U in the presence of urea too. It should be noted that it was important to demonstrate the hyperfluorescence of W53 in I_U for unfolding in urea too because there is experimental evidence showing that urea, but not GdnHCl, directly binds to peptide bonds,[35] and it was therefore possible that the structure of I_U is different for unfolding in urea and for unfolding in GdnHCl. In this context, it has been shown previously that the structure of the transition state for the unfolding of barstar in urea is significantly different from that for unfolding in GdnHCl.[36] The observation made in the current study that the spectroscopic properties of I_U are essentially the same in both GdnHCl and urea suggests that the rearrangement of tertiary contacts that enables the partial burial of W53 in I_U should also be independent of the denaturant used. Consequently, a molecular dynamics simulation approach was used to understand the nature of tertiary contacts that stabilize this transient partial burial of W53 in I_U.

Partial Burial of W53 during the Multistage Unfolding of the PI3K SH3 Domain in Urea. Multiple unconstrained MD simulations of the PI3K SH3 domain solvated in a box of aqueous 8 M urea solution were performed and analyzed by the simultaneous use of multiple measures to enable a detailed multidimensional characterization of this process. The experimentally observed unfolding time is ∼seconds with the formation of I_U occurring in less than a few milliseconds. Given the size of the system, it is challenging to perform full unfolding simulations under experimental conditions, as the unfolding time is dominated by the waiting time (in a free energy minimum) that is much longer than the time to cross the free energy barrier. Therefore, we performed simulations

dx.doi.org/10.1021/jp410019f | J. Phys. Chem. B XXXX, XXX, XXX−XXX

both at room temperature (300−310 K) and at elevated temperature (400−450 K). Details of these simulations are tabulated in Table 1. Briefly, eight different simulations were performed in 8 M urea, five (runs 1−5) at room temperature, and three (runs 6−8) at high temperature. The simulations were carried out for 500 ns or longer, and the total aggregate simulation time was ∼4.4 μs. Complete unfolding of the protein was observed in only one trajectory at 310 K and in two of the high temperature trajectories (run 4, run 7, and run 8, Table 1, see also discussions below). Nevertheless, the simulations performed in this study appear to capture an unfolding intermediate I_U and therefore can be used to provide molecular insights into the interactions of W53 with the rest of the protein at different stages of unfolding, leading to its hyperfluorescence. Figure 3a compares the distributions of the

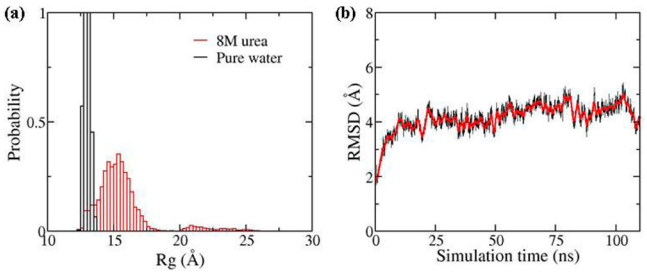

Figure 3. (a) Probability distributions of the distributions of the radius of gyration, R_g, of the protein in water (black) and in 8 M urea (red). The distribution in urea shown in a was obtained from an aggregate of ∼3.3 μs simulations performed at ∼300 K, whereas that in water was obtained from a ∼100 ns simulation at 300 K. (b) The evolution of the root-mean-square deviation, RMSD (Cα atoms only), from the native structure during a ∼100 ns simulation in water at 300 K, showing a plateau at ∼4 Å after 20 ns (black, raw data; red, moving average of 1 ns).

radius of gyration, R_g, of the protein in water and in 8 M urea. The distribution in urea shown in Figure 3a was obtained from an aggregate of ∼3.3 μs simulations performed at ∼300 K, whereas that in water was obtained from a 100 ns simulation at 300 K. Figure 3a suggests that the protein remained fairly folded in water with an average R_g value of ∼13 Å. In contrast, the protein explores various unfolded conformations in urea (the observed largest R_g value was 27 Å). The RMSD plateaus to ∼4 Å after 20 ns of simulation (Figure 3b), suggesting that the protein structure remains fairly stable in water. When the simulation was, however, carried out, at an elevated temperature (500−600 K), full unfolding was observed in pure water (see later).

The simulations were then used to determine whether, when, and how W53 becomes transiently buried during urea-induced unfolding, as observed in the experiments. Results from all eight runs in aqueous 8 M urea are shown in Figures 4 and Figures S1−S7 (Supporting Information). Figure 4c shows the evolution of the solvent-exposed surface area (SASA) of the W53 side chain, as well as of the C_α-RMSD during a ∼0.8 μs trajectory at 310 K (run 4). The evolution of the W53 side chain SASA alone is shown in Figure S8 (Supporting Information). In the native state, the SASA of the side chain of W53 is ∼140 Å^2, implying a solvent-exposed side chain. Figure 4c suggests that W53 undergoes partial burial at different stages of unfolding, consistent with the experimentally observed hyperfluorescence of W53 as described above. While details vary, all trajectories consistently show W53 burial during different stages of unfolding.

The first transition to a partially buried state (SASA ≤ 75 Å^2) is evident at a shorter time scale (∼50−80 ns) in a native-like ensemble (RMSD ≤ 6 Å), that is short-lived. This ensemble is referred to as I* hereafter. All of the trajectories show transient drop(s) in W53 SASA in I* (see Figures S1−S7, Supporting Information). W53 becomes re-exposed to solvent at ∼100 ns as I* gradually unfolds further. At a much longer time scale (>300 ns), a partially unfolded, long-lived intermediate ensemble (referred to as I_U in experimental studies[18,26]) is populated with an RMSD of ∼12 Å. In this intermediate, W53 undergoes transitions between partially buried and solvent-exposed states in run 1, run 4, run 5, run 6, and run 8. Interestingly, run 3 and run 7 show an I_U population with no significant W53 burial (see later). The probability of finding W53 buried in the simulated I_U ensemble is ∼10.7 ± 1%, estimated from a loosely defined I_U ensemble consisting of 153 880 conformations with 6 Å < RMSD < 16 Å. The fluctuations in the SASA of W53 in this state are much larger than what is observed in I*, suggesting that the environment around W53 is more plastic in I_U than in I*. The I_U population is also noticed in high temperature simulations (run 6 and run 8, see Table 1, and Figures S5 and S7, Supporting Information). In experiments, the transient burial of W53 in I_U was found to be accompanied by a relatively small blue shift in the λ_{max} of W53 fluorescence,[18] but it could not be determined whether the shift was due to W53 becoming partially buried in all I_U molecules or due to W53 becoming fully buried in only a fraction of I_U molecules. The simulations indicate that the latter is true.

The I_U ensemble eventually unfolds to the fully unfolded state, U (with RMSD > 16 Å). I_U is a structurally loose ensemble, in which the majority of the native contacts are broken and a significant amount of secondary structure is disrupted. I_U is much longer-lived than I* (see also Figures S1−S7, Supporting Information), suggesting that most of the W53 hyperfluorescence seen in experiments is contributed by the I_U ensemble. The value of R_g is seen to increase up to 24 Å, while the value of Q reduces to around 0, which is expected for the U state. W53 is found to be transiently and infrequently buried also in the U ensemble. Thus, the conformational ensemble in which W53 can be partially buried is structurally heterogeneous and is populated at different stages of unfolding. A comparison with the evolutions of the W53 SASA and RMSD during a thermal unfolding simulation at 500 K (Figure S9a, Supporting Information) reveals that both heat and urea denature the PI3K SH3 domain in a similar manner: native-like I* structures are visited early with a later population of partially unfolded I_U conformations.

The evolution of R_g (Figure 3a) further suggests that the initial I* ensemble, in which W53 is buried, is highly compact in nature (R_g ∼ 13−14.5 Å). Hence, I* is slightly swollen compared to the native state ($Q \geq 0.75$), whose R_g is ∼12−13 Å, but mainly native-like as suggested by RMSD (≤6 Å). In contrast, the longer-lived I_U ensemble is structurally loose with R_g ∼ 16 Å. The U ensemble has an overall much higher R_g value (∼21 Å), although transient drops to lower values, suggesting nonspecific collapse, are often noticed. The evolution of Q (Figure 4b) further confirms that I* has native-like structure ($Q \approx 0.6$), whereas I_U is more unfolded ($Q \approx 0.4$). Thus, the conformational ensemble in which W53 can be partially buried is structurally heterogeneous.

dx.doi.org/10.1021/jp410019f | J. Phys. Chem. B XXXX, XXX, XXX−XXX

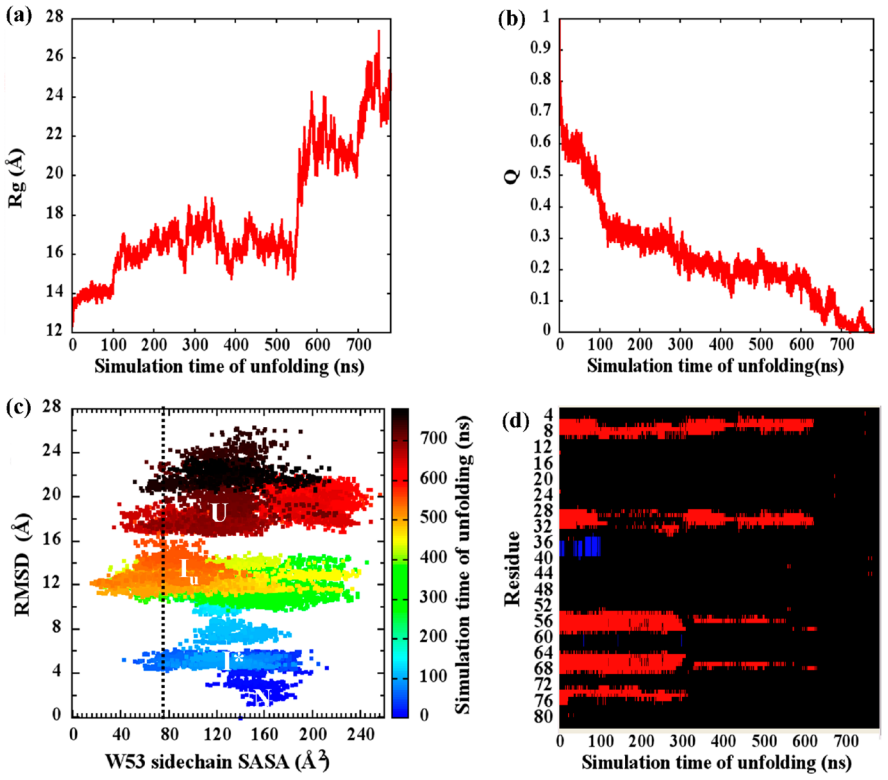

Figure 4. Simulation data showing partial burial of W53 at different stages of the unfolding of the PI3K SH3 domain in 8 M urea at 310 K (run 4 in Table 1). Panels a and b show the time dependences of the radius of gyration, R_g, and of the fraction of native contacts, Q, respectively. Panel c shows the evolution of the solvent-exposed surface area, SASA, of the W53 side chain and of the root-mean-square deviation, RMSD ($C\alpha$ atoms only), from the native structure during a typical 800 ns trajectory. Each point on this plot is colored according to its time of occurrence with the color scale shown. The solid black line at W53 SASA = 75 Å^2 defines the partially buried states. Panel d shows the evolution of secondary structure (red = β-strands, blue = helices, black = coils).

It should be noted that I* has not been detected in earlier experimental studies.[18,26] This is probably because it is formed very early (<100 ns in simulations) in the unfolding reaction. Moreover, simulations show that I* is extremely short-lived (~ns) and quickly transits to the I_U ensemble. A comparison with the simulation results performed in water (Figure 3) further confirms that native-like but slightly swollen I* structures are populated en route during an early stage of urea-induced denaturation but not in water at 300 K. However, during a thermal unfolding simulation, conformations similar to I* are found to be populated (Figure S9, Supporting Information).

Unfolding of the PI3K SH3 Domain Occurs Non-cooperatively. Exploring the cooperativity of the structural changes during the unfolding reactions of small proteins has been a challenge in experiments, due to the limited sensitivity of the probes commonly used. The use of multisite time-resolved fluorescence resonance energy transfer (FRET) probes has, however, shown that unfolding reactions can be so highly noncooperative that they occur in a gradual manner, both in the case of barstar[37] and monellin.[38] In the case of the PI3K SH3 domain, hydrogen exchange-mass spectrometry (HX-MS) studies[27] have suggested that unfolding at low GdnHCl concentration is gradual in nature, and that at higher GdnHCl concentration at least one unfolding intermediate is populated. The results of the simulations presented above show that the burial of W53 can occur on different time scales during the urea-induced unfolding of the protein, consistently implying that the reaction is noncooperative and is not all or none. The comparison of the urea unfolding results with the thermal unfolding data (Figure S9, Supporting Information) suggests that heat unfolds the protein in a manner similar to how urea does: a short-lived native-like early intermediate, similar to I* in urea, is first formed, followed by population of a longer-lived more unfolded I_U intermediate. On the basis of this result, it can be concluded that urea does not make the unfolding more noncooperative, and that both I* and I_U are en route unfolding intermediates.

The evolution of secondary structure, calculated using the program STRIDE,[39] was computed to understand better the structural details of the unfolding process. Figure 4d shows that the secondary structure of the protein remains fairly undisrupted up to 100 ns, despite the fact that Q decreases to ~40%. As unfolding progresses, the C-terminal β-strands (mainly β3 and β4) become strongly disrupted in the I_U state, whereas the β1 and β2 strands stay mostly intact. This trend was found in all trajectories that show an I_U population with W53 burial (see Figures S1−S7c, Supporting Information). However, the two trajectories that exhibit no significant burial of W53 in the I_U state (run 3 and run 7) show structural weakening of the N-terminal β-strand(s) before the C-terminal ones (Figures S3c and S6c, Supporting Information). These results strongly suggest the presence of significant structural heterogeneity in the I_U state (see later). For this reason, those two runs (run 3 and run 7) with distinct I_U structures were analyzed and discussed separately from the remaining trajectories. The unfolded U ensemble lacks any significant secondary structure.

dx.doi.org/10.1021/jp410019f | J. Phys. Chem. B XXXX, XXX, XXX−XXX

Also computed were the changes in the native tertiary contact probabilities for the N → I* → I_U process. The contact probabilities (Q_{ij}) were estimated by ensemble averaging (N = 0.75 ≤ Q ≤ 1; I* = 0.5 ≤ Q ≤ 0.75; and I_U = 0.5 ≤ Q ≤ 0.25) using the conformations obtained from all trajectories except run 3 and run 7. The Q-based criterion used to define each ensemble is somewhat arbitrary, as the N → I* → I_U transition appears to be gradual (see later). These results are depicted in Figure 5. The native contact probabilities for each ensemble

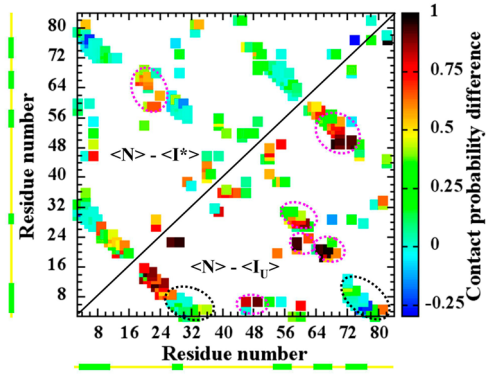

Figure 5. Changes in the probabilities of native contact formation for the I* state (above the diagonal) and the I_U state (below the diagonal) from the native state, N. The probabilities were estimated by ensemble averaging (N = 0.75 ≤ Q ≤ 1, I* = 0.5 ≤ Q ≤ 0.75, and I_U = 0.25 ≤ Q ≤ 0.5) using the conformations obtained from multiple trajectories (a total of ∼350 000 conformations from run 1, run2, run 4, run 5, run 6, and run 8 are used for this analysis). Tertiary long-range contacts that are disrupted are circled in purple, and the ones maintained are circled in black. The locations of β-strands (green boxes) are also shown along the sequence (yellow line) drawn along each axis.

(N, I*, I_U, and U) are also shown in Figure S10 (Supporting Information). Figure 5 implies that the disruption of tertiary native contacts as the protein unfolds from N to I* to I_U is gradual. The unfolding is initiated with the weakening of the long-range native contacts between the N-terminal strands (β1 and β2) and the residues 56−68 (β3 and β4). For all those contacts, the probability of formation decreases from the N state by a value of ≥0.5. Weakening of contacts is also observed in I* between residues 49−54 and residues 66−70, which becomes more prominent in I_U. Figure S10 (Supporting Information) suggests that, even in the N ensemble, the nSrc loop is unstructured. These results are in good agreement with previous hydrogen−deuterium exchange (HX) measurements, which suggested that the unfolding of the PI3K SH3 domain begins from residues 1−13, residues 37−51, and residues 52−72 in 1.8 M GdnHCl.[27] In the I_U ensemble, the contacts between β1, β2, and β5 (circled in black in Figure 5) are maintained ($Q_{ij}^{\langle N\rangle} - Q_{ij}^{\langle I_U\rangle} \leq 0.25$), suggesting that this core is preserved. The simulation results (Figure 5 and Figure S10, Supporting Information) combined with the previously reported HX measurements suggest that the unfolding of the PI3K SH3 domain is gradual in nature, and begins with loosening of the tertiary, long-range, native contacts (contacts between β1 and β2 as well as between β3 and β4), while the β1, β2, and β5 strands maintain a core in the trajectories that exhibit W53 burial in the I_U state. In contrast, results from run 3 and run 7 suggest that W53 remains in a locally more native-like environment in the I_U conformations populated in those trajectories.

The experimental observation that the hyperfluorescence of W53 in I_U increases monotonously in a nonlinear manner with an increase in urea concentration (Figure 2c) also indicates that unfolding from N to I* to I_U is noncooperative and might be gradual in nature. It should be noted that the N to I_U transition monitored using tyrosine fluorescence does show an apparently sigmoidal dependence on urea concentration, but a sigmoidal dependence of such a burst phase transition is not necessarily indicative of a cooperative transition.[28,40−44] When unfolding is carried out in GdnHCl, the increase in the hyperfluorescence of W53, as well as in the fluorescence of ANS when bound to I_U which accompanies the N → I_U transition, also increases in a nonlinear monotonous manner with an increase in GdnHCl concentration, again suggesting that this transition is gradual in nature.[18] In this context, it should be noted that the structure of the N state also appears to be malleable, with the content of its secondary structure changing significantly with the addition of a stabilizing salt.[29] Our results support the emerging view that incremental loss (gain) of side chain packing can result in a progression of discrete intermediates in protein unfolding (folding) reactions (see ref 31 and references therein), which calls for a re-evaluation of the simple two-state resulting in the noncooperative nature of the model of protein unfolding/folding reaction.

Properties of I_U from Experiments and Simulations Identify It as a Wet Molten Globule. Earlier experimental studies performed at high concentrations of denaturant and using optical probes showed that the unfolding of the PI3K SH3 domain could be explained by invoking an intermediate ensemble, I_U.[26] A detailed kinetic analysis also showed that I_U is populated after the rate-limiting step during refolding. The same study used the fluorescence from seven Tyr residues distributed in the sequence to probe for changes in tertiary structure and used far-UV CD at 222 nm to probe for changes in secondary structure during unfolding. These probes showed that I_U resembles a wet molten globule in having U-like Tyr fluorescence but N-like secondary structure. Moreover, it was shown that only about 55% of the overall SASA becomes buried in I_U during refolding, indicating that it does not have a very rigid structure.[26] The properties of the I_U ensemble obtained from the simulations are in overall agreement with those obtained from experiments (see above). I_U is a structurally loose (molten globule) ensemble, in which a majority (∼60%) of the native contacts is broken, and a significant amount of secondary structure is disrupted. In addition, the tyrosine residues are seen to be mainly solvent-exposed in the simulated I_U state (see Figure S11, Supporting Information), which is in agreement with previous experimental data that indicated that the tyrosine fluorescence of I_U is the same as that of U.[26]

The observation that the fluorescence of W53 in I_U decreases in a monotonous, nonlinear manner with a decrease in urea concentration (Figure 2c) can also be interpreted to indicate that the I_U ensemble is a conformationally heterogeneous ensemble.[18,29] It appears that a denaturant or heat induced conformational interconversion can occur within the I_U ensemble as a result of increased conformational entropy, with each subpopulation differing in the extent to which W53 is buried (see Figure 4c and Figure S9a, Supporting Information). Consistently, the simulation results presented here also demonstrate the broad fluctuation in the SASA of W53 (see Figure 4c) within the I_U ensemble. In addition, the simulations highlight structural heterogeneity within the I_U ensemble (see

dx.doi.org/10.1021/jp410019f | J. Phys. Chem. B XXXX, XXX, XXX−XXX

the section below on the requirement of W53 burial in the I_U ensemble for unfolding).

Long-Range Interactions Leading to Burial of W53 during Unfolding. Contact formation between W53 and the rest of the protein was computed as a function of time of unfolding, in order to identify the residues contributing to its partial burial. Residues *i* and *j* are deemed to be in contact if any heavy atom of residue *i* is within 5 Å of any heavy atom of residue *j*. Figure 6a shows the set of residues interacting with the side chain of W53 at different stages of the unfolding reaction. Results from the other seven trajectories are shown in Figures S1−S7 (Supporting Information). In addition, typical snapshots of the local environment of W53 (buried or exposed) in different ensembles (I*, I_U, or U) are shown in Figure 6b. In the N state, the solvent-exposed W53 has been shown by NMR to be in contact with residues D19, D66, F67, and P68. In the native-like I* ensemble, the side chain of W53 forms long-range contacts mainly with two sets of residues: residues 12−24 (RT loop) and residues 66−71 (β5 strand), which involves hydrophobic (e.g., with Y12, F67, and P68) as well as van der Waals forces. One snapshot at 60 ns (Figure 6b) shows the conformation in which W53 is partially buried due to interactions with Y12. The relative orientations of W53 and Y12 rule out the possibility of $\pi-\pi$ interactions. Thus, predominantly hydrophobic forces appear to promote the W53−Y12 interaction. The unfolding of I* is accompanied by disruption of many of those contacts. The conformation at 160 ns, with W53 getting re-exposed, and in which the contacts with the RT loop are disrupted (Figure 6b) supports this result. The unfolding of I* results in the re-exposure of W53, which is accompanied with a significant change in the tertiary structure of the protein (resulting in a further decrease in *Q* from 0.4 to <0.3; Figure 4b).

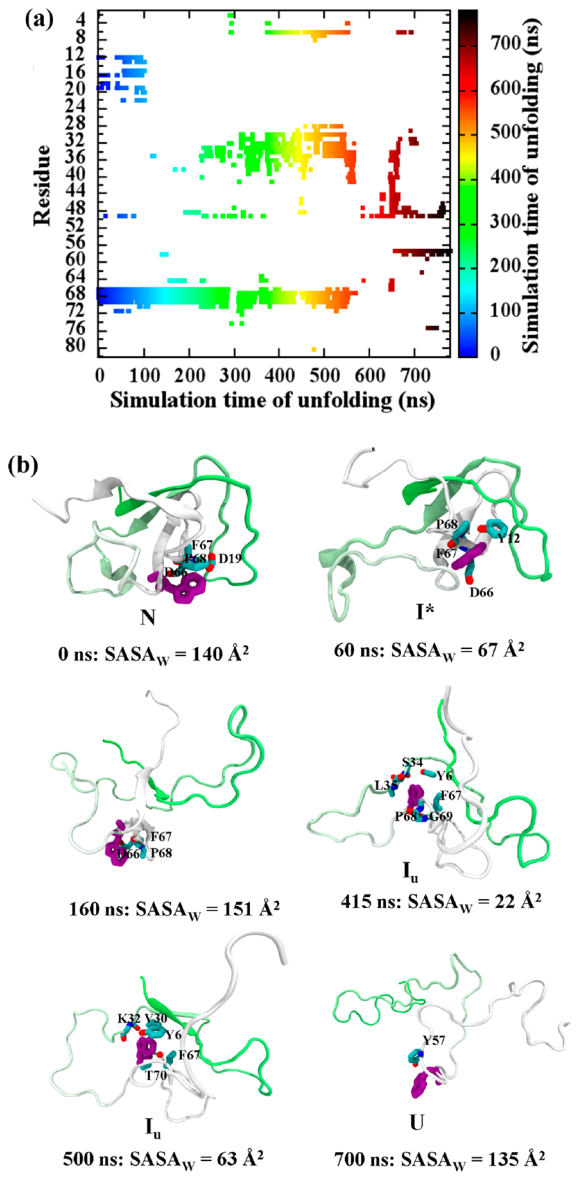

Figure 6. Panel a shows the evolution of W53 contacts with the rest of the protein during run 4 (Table 1). A contact is considered if heavy atoms of two residues are within 5 Å of each other. Only tertiary interactions are shown ($|i - j| > 3$). Panel b shows snapshots of I*, I_U, and U states from the trajectory. The protein is shown using a cartoon representation. The color scale used is green to white (N-terminal to C-terminal). W53 and the residues in contact with it are shown in licorice representation. The W53 side chain is shown in purple, whereas the following colors are used for the contacting atoms: C = cyan, O = red, N = blue.

Interestingly, as unfolding progresses, a completely different set of contacts with W53, which are non-native in nature, emerges in the I_U ensemble ($0.25 \leq Q \leq 0.5$). Such contacts involve residues 26−49 from the nSrc loop and residues 1−6 from the β1 strand. The residues that form contacts with the buried W53 side chain in the I_U ensemble with >20% probability are A1, Y6, V30, N31, K32, G33, S34, L35, and V36. These contacts can be classified into medium-range ($3 < |i - j| < 10$) and long-range ($|i - j| \geq 10$) contacts. A similar classification of contacts within a protein structure has been used previously.[45,46] Clearly, most of the contacts formed by W53 in I_U are long range in nature. A major fraction of those residues involved in long-range contacts with W53 are hydrophobic in nature. Snapshots of the I_U conformations with a partially buried W53, from the trajectory, support this observation (Figure 6b). Thus, the formation of long-range, non-native contacts with a cluster of hydrophobic residues underlies the burial of W53 in the long-lived I_U state.

As mentioned above, W53 may be partially buried even in the U state ($Q \leq 0.25$). However, the burial occurs less persistently and infrequently compared to what is observed in I_U, which is likely due to the lack of structure and to the greater conformational freedom of the chain in U. The residues that form transient contacts with the buried W53 in the U state with >20% probability are F40, E45, A46, K47, and P48. Thus, the transient and infrequent burial of W53 in the U state is primarily accompanied by the occasional formation of medium-range contacts with the nSrc loop.

Residual Contacts in U. In a previous experimental study of the folding of the PI3K SH3 domain, refolding was shown to begin by the nonspecific collapse of the unfolded state to a structure-less globule.[28] In that study, although the far-UV CD spectrum of the GdnHCl-induced unfolded state exhibited features of a random coil state, multisite FRET measurements on the unfolded state of the protein indicated that intramolecular distances were close in value to those calculated for an unfolded polypeptide chain modeled as a random coil but only when the excluded volume effect was not accounted for.[47] This suggested the existence of residual structure in the unfolded state. This residual structure may be tertiary in nature, which is a result of the constantly changing environment of the

dx.doi.org/10.1021/jp410019f | J. Phys. Chem. B XXXX, XXX, XXX−XXX

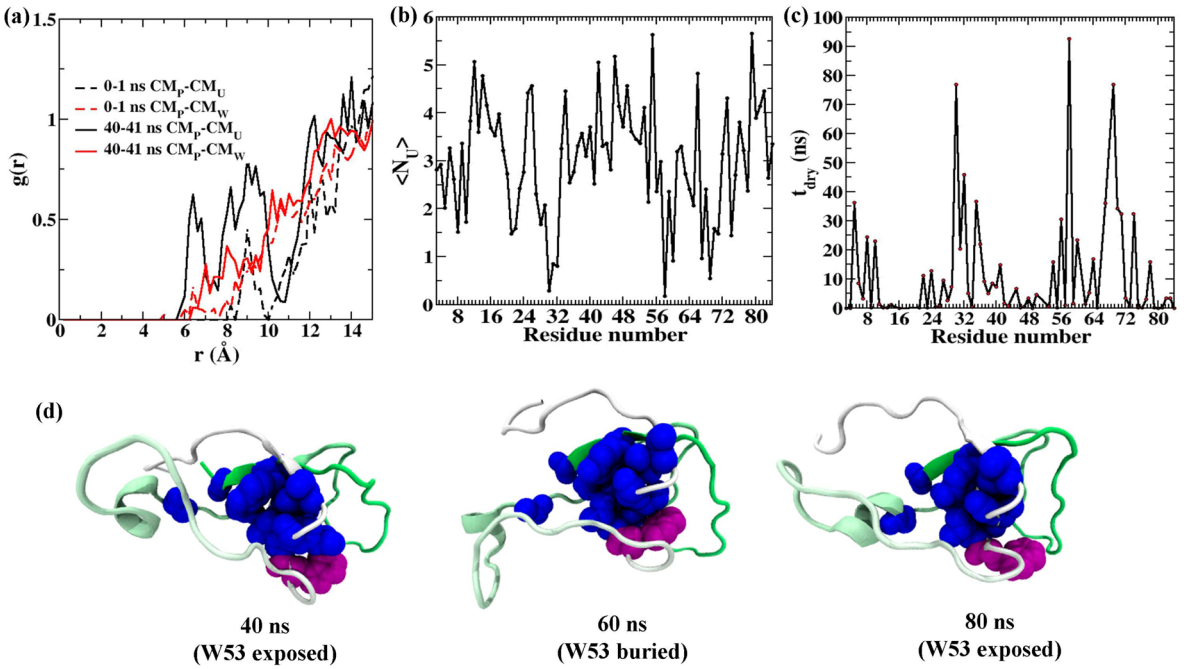

Figure 7. Characteristics of the initial molten globule state I*. Panel a shows the radial distribution functions between the center of mass (CM_X) of a urea/water molecule and the (CM_P) of protein at 0−1 and 40−41 ns of unfolding during run 4 (Table 1). Panel b shows the number of urea molecules in contact for each residue averaged over the first 100 ns of simulation. A solvent molecule is considered in the FSS if any heavy atom of the solvent is within 4 Å of the dry residues (heavy atoms only). Panel c shows the time spent in the dry state ($N_w \leq 1$, where N_w is defined by the number of water molecules within 4 Å of a particular residue). The data shown is averaged over the first 100 ns of the trajectory. Snapshots of the "dry" residues are depicted in panel d. A total of 12 dry residues, i.e., G3, Y6, L28, V30, G33, L54, G56, G65, F67, P68, G69, and V72, are shown as van der Waals spheres in blue. W53 is also shown in purple.

aromatic residues (Trp, Tyr, and Phe) as the protein unfolds.[48] In the simulations, transient drops in R_g for the unfolded state ensemble are consistently observed (Figure 4). Some native-like packing between the β1 and β2 strands and/or between the β3 and β4 strands may persist even in the U state (Figure S10c, Supporting Information).

In addition, the formation of medium-range interactions between W53 and the hydrophobic residues in U is observed, resulting in the infrequent partial burial of W53 (Figure 6). Residual structure observed in the denatured states of several proteins[49,50] has been suggested to arise due to the formation of hydrophobic clusters (native or non-native).[51−53] Medium/long-range, non-native, residual attractions between hydrophobic residues have been shown to form transiently, even in expanded unfolded forms lacking any secondary structure.[46] In fact, non-native secondary structure was shown to populate compact conformations of the denatured state of the SH3 domain of α-spectrin.[54] Hydrophobic clusters in the unfolded state may serve as nucleation sites for the formation of structure during folding,[55,56] and the folding of the src SH3 domain,[57] and recently the folding of both the Fyn and PI3K SH3 domains[58] has been shown to commence with the formation of non-native secondary structure.

Is W53 Burial in the I_U Ensemble a Requirement for Unfolding? In the I_U ensemble, strands β1, β2, and β5 mostly maintain their structure, while the rest of the protein becomes unfolded and conformationally flexible (Figures 4 and 5). All seven tyrosine residues become solvent-exposed in the I_U state (Figure S11, Supporting Information). The conformational flexibility of the partially unfolded I_U ensemble enables the transient burial of W53 by allowing it to form non-native contacts with hydrophobic residues from the nSrc loop and the N-terminus of the β1 strand. It appears, however, that the burial of W53 is not a requirement for unfolding. For instance, run 3 (at 300 K) and run 7 (at 425 K) show unfolding through intermediate structures that do not experience W53 burial. In those trajectories, unfolding begins with the disruption of the β1 and/or β2 strands from the rest of the protein (Figures S3 and S7, Supporting Information). As a result, the I_U ensemble shows much less W53 burial due to the absence of long-range interactions. This is because the β3 and β4 remain structured, thereby not allowing W53 to become buried in the I_U ensemble (Figures S3 and S7, Supporting Information). This finding shows that the burial of W53 within a specific I_U conformation is strongly related to the detailed structure of the protein. Nevertheless, the transient burial of W53 in the I* state, accompanied by interactions with the RT loop, is noticed in those trajectories (Figure S12, Supporting Information), suggesting that the structural heterogeneity in I* is much less compared to I_U.

Initial Dry Nature of the Transient Molten Globule State I*. Transient burial of W53 is observed to occur first in the I* ensemble, which is native-like and structurally compact, and which has most of the secondary structures intact. The I* ensemble has, however, significantly lost tertiary interactions. Such structural features of I* are characteristic of a molten globule state. It was important to determine whether the side chains buried in the hydrophobic core have become hydrated in I*, or whether the hydrophobic core is dry as in a dry molten globule (DMG). Both experiments and simulations have suggested the existence of an early DMG intermediate, with native-like secondary structure and with a hydrophobic core that has not yet become hydrated, during the unfolding of small proteins.[31,32] To test the wet/dry nature of I*, the population

dx.doi.org/10.1021/jp410019f | J. Phys. Chem. B XXXX, XXX, XXX−XXX

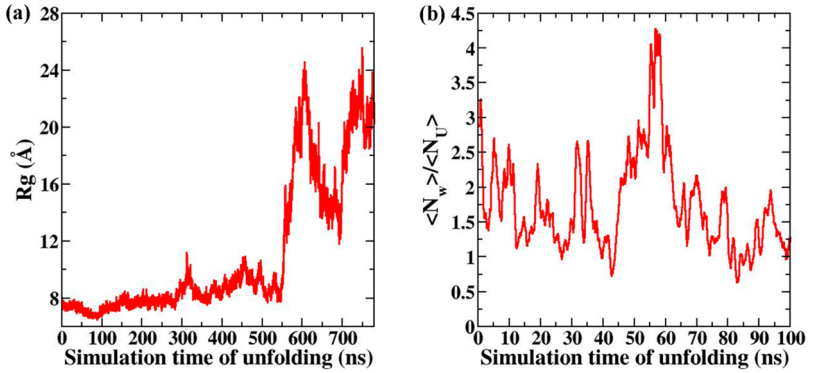

Figure 8. Panel a shows the C_α radius of gyration, R_g, of the dry residues during the unfolding reaction. Panel b shows the ratio of urea to water in the first solvation shell (FSS) of the dry residues during the first 100 ns. A solvent molecule is considered in the FSS if any heavy atom of the solvent is within 4 Å of the dry residues (heavy atoms only). The data shown is block-averaged over a 1 ns window. Data from run 4 (Table 1) has been used for the analysis presented here.

of urea/water molecules inside the protein core of I* was characterized. For this, the radial distribution function between the center of mass of a urea/water molecule (CM_U/CM_W) and of the protein (CM_P) at 0−1 ns and at 40−41 ns of unfolding (Figure 7a) was computed. The density of urea increases much faster than water within the protein core (10 Å), suggesting that urea penetrates the protein core in I* before water does.

As shown in Table 1, DMG formation is seen in all of the eight trajectories performed at different temperatures (see Figure S13, Supporting Information). The core of the initial molten globule I* appears to remain dry for up to ∼40−50 ns at ∼300 K during unfolding; nevertheless, the denaturant molecules can penetrate the core. The preferential penetration of urea is associated with the subtle swelling of the structure (suggested by the evolution of R_g shown in Figure 4a) and weakening of tertiary native contacts (contacts between β1 and β2 as well as between β3 and β4). The first observation of an initially formed transient DMG intermediate, using simulations, was reported for the urea-induced unfolding of the hen egg lysozyme.[32] The present study reports a similar urea-filled DMG intermediate during the unfolding of the PI3K SH3 domain. Lysozyme and the PI3K SH3 domain have significant structural differences: (a) 129 residues versus 82 residues, (b) predominantly α-helical versus β-sheet rich protein, (c) two domains versus a single domain, respectively. The results presented here, combined with those reported earlier[32] and previous experimental observations,[31] support the formation of the DMG intermediate during the early stages of the denaturant-induced protein unfolding, as a general molecular mechanism. Such preferential intrusion of urea into the dry protein core has been attributed to the stronger van der Waals (vdW) interaction of urea with the hydrophobic core of the protein.[16,32,59] This interaction results in the preferential accumulation of urea in the first hydration shell of the protein, as suggested by the evolution of the ratio of water to urea, $\langle N_W\rangle/\langle N_U\rangle$, in the first solvation shell (FSS) of the protein (Figure S14a, Supporting Information). Within the first 15 ns, the value of $\langle N_w\rangle/\langle N_U\rangle$ drops from 4 to 2.5 and then fluctuates between 2 and 3. For comparison, the $\langle N_W\rangle/\langle N_U\rangle$ is 4.3 in the bulk. This result suggests that the concentration of urea constantly remains about 2 times higher in the first solvation shell of the protein compared to the bulk during unfolding. Further decomposition of the ratio in terms of protein residue type (hydrophobic, polar, and charged) reveals a consistently smaller value of $\langle N_W\rangle/\langle N_U\rangle$ near the hydrophobic residues compared to the polar and charged ones, suggesting that during the full time course of the unfolding reaction urea preferentially interacts with hydrophobic residues. We also plotted the time dependence of the number of hydrogen bonds (backbone−backbone, backbone−urea, and backbone−water) in Figure S14b (Supporting Information). An initial decrease in the number of backbone−backbone hydrogen bonds from ∼30 to ∼20 is noticed during the first ∼20 ns. During this time, the protein swells to a R_g value of 14 Å. On this time scale, the number of backbone−urea hydrogen bonds increases from ∼40 to ∼56, whereas the backbone−water hydrogen bonds remain nearly constant. An increase in backbone−water hydrogen bonds is observed after the first ∼40 ns. This result is consistent with the mechanism in which urea−backbone interaction results in the swelling of the protein core followed by water penetration. Following this initial phase, the intraprotein hydrogen bonds decrease gradually. The number of backbone−urea hydrogen bonds fluctuates around an average value of ∼60, whereas the backbone−urea hydrogen bonds fluctuate around an average value of ∼88. This result implies that the denaturing action of urea is further augmented by preferential hydrogen bond formation with the protein backbone. Nevertheless, hydrogen bonding alone cannot direct urea-induced protein unfolding. In that case, more prevalent interactions between urea and polar residues of protein would be expected, which is clearly not the scenario presented here (see Figure S14a, Supporting Information), and also for a number of other proteins.[32,60,61]

Figure 7b shows the average number of contacting urea molecules per residue in I* during the first 100 ns. The top 10 residues in terms of urea binding tendency are Y12, Y14, L26, K34, F42, Q46, K49, W55, R66, and R79, suggesting preferential binding of urea with residues that have either hydrophobic or bulky side chains. To gain detailed insight into the residue-specific dryness of I*, t_{dry}, the time spent by each residue in the dry state during the first 100 ns of unfolding was computed (Figure 7c). A residue is considered dry at any time t if $N_W \leq 1$, where N_W is the number of water molecules within 4 Å of the heavy atoms of that particular residue. If residues are considered "dry" residues when $t_{dry} \leq 25$ ns, then a total of 12 residues have to be considered, i.e., G3, Y6, L28, V30, G33, L54, G56, G65, F67, P68, G69, and V72. The majority of the dry residues are hydrophobic (both aliphatic and aromatic) and constitute the dry interior of the initial molten globule state, I*. Figure 7d displays snapshots of these dry residues at 40−60 ns

dx.doi.org/10.1021/jp410019f | J. Phys. Chem. B XXXX, XXX, XXX−XXX

of unfolding, revealing the compact nature of the dry core of the PI3K SH3 domain. It should also be noted that the initially formed, transiently populated, urea-filled dry core appears to be an intrinsic feature of the I* molten globule, as it is also observed in the trajectory that unfolds via structurally different I_U conformations, that do not show significant W53 burial (see Figure S10, Supporting Information). It must be mentioned that the initial swelling of the protein, while maintaining its native-like structure, is also observed in thermal unfolding simulation (Figure S9b−d, Supporting Information). Such swelling is observed even before water penetrates the protein core (∼25 ns), suggesting that the DMG-like structures are transiently populated also during thermal unfolding.

Nature of the Transient W53 Burial within the Native Hydrophobic Cluster of I*. The time dependence of $C_\alpha-R_g$ of these dry residues was computed during the 700 ns of unfolding (Figure 8a), to check how long this core is maintained during unfolding. The $C_\alpha-R_g$ of the dry residues remains unchanged until ∼40 ns. A slight decrease of $C_\alpha-R_g$ during 40−80 ns of unfolding suggests that the dry core becomes more tightly packed. Interestingly, transient burial of W53 also occurs at this time. Subsequently, an increase of $C_\alpha-R_g$ to ∼8 Å is observed, which remains constant until the protein unfolds completely.

An estimate of how the ratio $\langle N_W\rangle/\langle N_U\rangle$ in the first solvation shell (FSS) of those dry residues changes during the first 100 ns of unfolding is displayed in Figure 8b. An overall decrease of $\langle N_W\rangle/\langle N_U\rangle$ from 3.25 to <1 in the first ∼40 ns supports the conclusion that urea intrudes into the core ahead of water. The drop in $C_\alpha-R_g$ at ∼40−80 ns coincides with an increase in water with respect to urea around those dry residues. The data suggest that after ∼40 ns water starts to intrude into the core. At this time, the occasional enhanced population of water, due to solvent density fluctuations, inside the hydrophobic core of the protein can trigger a transient and slight collapse. This collapse appears to promote the partial burial of W53 initiated by a subtle side chain reorganization of the native hydrophobic cluster (e.g., residues from the RT loop). The burial of W53 in I* is much more transient compared to what is observed in I_U.

An important question is whether I* is a discrete thermodynamic state or not. The observations from both experiments and simulations (see above) showing that the unfolding of N to I_U via I* is a gradual process suggest that the hydration of the core hydrophobic residues is not an all-or-none process, and that I* may not be a discrete state. In order to validate this *in silico*, it will be necessary to define the free energy landscape for the protein unfolding reaction in aqueous urea using multiple reversible folding/unfolding equilibrium trajectories. Given the size of the protein and the time scale of the process (∼milliseconds), such calculations will be computationally expensive with the currently available resources. An alternative way is to perform accelerated molecular dynamics methods such as replica exchange. However, crucial kinetic information such as preferential intrusion of urea into the protein core may then be missed.

CONCLUSIONS

The molecular interactions underlying the transient partial burial of W53 during the unfolding of the PI3K SH3 domain in aqueous urea have been delineated in detail, using a combined experiment−simulation approach. Experiments revealed a transient hyperfluorescence of W53 during unfolding in urea, implying a transient, non-native burial of W53. A consistent, partial burial of W53 within a cluster of hydrophobic residues at different stages of unfolding in 8 M urea was also observed in simulations. In the early stages of unfolding, the initially solvent-exposed W53 is transiently and partially buried in a native-like molten globule state I*. A dry urea-filled core is observed in I* at $t \leq 50$ ns during unfolding, suggesting population of dry molten globule (DMG)-like structures. Urea enters the hydrophobic core of the protein before water, resulting in a dry urea-filled core in I* at the very earliest stages of unfolding. When water starts to penetrate the core, subtle side chain reorganization of the native hydrophobic core allows burial of W53 in I*. Interactions between W53 and the hydrophobic residues (e.g., Y12) from the RT loop (in addition to those with the β5 strand which were originally present in the native state) help to initiate the transient burial.

W53 is found to experience a stronger and more consistent partial burial in a subsequent partially unfolded intermediate state I_U that is seen to form in experiments and is a wet molten globule in nature. The I_U ensemble is conformationally heterogeneous in nature, and W53 burial in a specific I_U conformation strongly depends on the detailed structure. The environment of W53 in I_U also appears to be structurally plastic. Simulations reveal that the majority of I_U conformations with an intact hydrophobic core consist of β1, β2, and β5, while the rest of the protein is unstructured. This partial unfolding of the local environment of W53 results in its non-native, tertiary interactions with hydrophobic residues from the N-terminal of the β1 strand (residues 2−8) and the nSrc loop (residues 26−49). Such non-native, tertiary contact formation with hydrophobic residues allows frequent burial of W53. Furthermore, it is found that W53 burial is likely not a requirement for unfolding, and rather a consequence of the structural heterogeneity of the I_U ensemble. In the I_U ensemble, a subset of conformations is found to have structurally intact C-terminal β-strands, in which the burial of W53 is not noticed. Thus, the simulations together with previous experimental results suggest that the non-native, long-range, hydrophobic interactions leading to the partial burial of W53 during the unfolding of the PI3K SH3 domain may serve to protect the protein from aggregation.

MATERIALS, METHODS, AND MODELS

Experimental Section. *Protein Expression and Purification.* The PI3K SH3 domain was purified as described previously.[26,28] Electrospray ionization mass spectrometry showed that the protein had an expected mass of 9276.2 Da. The sequence of the protein used is given below:

AEGYQYRALYDYKKEREEDIDLHLGDILTVNKGSLV-ALGFSDGQEAKPEEIGWLNGYNETTGERGDFPGTYV-EYIGRKKISP

Buffers, Reagents, and Experimental Conditions. All reagents and buffers of the highest purity grade were procured from Sigma. Ultrapure grade urea was obtained from USB Corp. Twenty mM phosphate buffer (pH 7.2) was included in the buffers used for all experiments, which were all performed at 25 °C. The concentrations of stock solutions of urea were determined by refractive index measurements on an Abbe refractometer. The concentration of the protein was determined by measurement of absorbance at 280 nm using ε = 17 900 M^{-1} cm^{-1}.[62]

For equilibrium unfolding experiments using Trp fluorescence as the probe, the concentration of the protein used was

dx.doi.org/10.1021/jp410019f | J. Phys. Chem. B XXXX, XXX, XXX−XXX

10−15 μM. For the kinetic unfolding experiments, using Trp fluorescence, the protein concentration used was 20 μM.

Equilibrium Unfolding Experiments. Fluorescence experiments were performed on a stopped-flow module (SFM-4, Biologic) in a fluorescence cuvette of 1 cm path length. The wavelength used for the selective excitation of Trp fluorescence was 295 nm, with a bandwidth of 4 nm. The fluorescence emission was measured through a 320 nm bandpass filter of bandwidth 10 nm (Asahi Spectra).

Kinetic Unfolding Experiments. All kinetic unfolding experiments, using Trp fluorescence as the probe, were performed using the SFM-4 stopped-flow module. Typically, a dead time of 6 ms was achieved with a cuvette of 0.15 cm path length.

Data Analysis. *Analysis of the Equilibrium Unfolding Data.* The equilibrium data for the unfolding of N to U, as a function of the concentration of urea, [D], was fit to a two-state N ↔ U model given by the following equation:

$$Y_0 = \frac{Y_N + m_N[D] + (Y_U + m_U[D])e^{-(\Delta G^\circ_{NU} + m_{NU}[D])/RT}}{1 + e^{-(\Delta G^\circ_{NU} + m_{NU}[D])/RT}} \quad (1)$$

where Y_0 is the value of the spectroscopic property being measured as a function of [D]; Y_N and Y_U represent the intercepts; m_N and m_U represent the slopes of the pre- and post-transition baselines for the N ↔ U transition, respectively. ΔG°_{NU} is the free energy of unfolding of the N state in water, and m_{NU} is the change in the free energy associated with the preferential interaction of [D] with the U state, relative to the N state.

The raw data for the equilibrium unfolding of N to U was also converted to plots of f_U (fraction unfolded) versus [D] using eq 2 and then fit to eq 3:

$$f_U = \frac{Y_0 - (Y_N + m_N[D])}{(Y_U + m_U[D]) - (Y_N + m_N[D])} \quad (2)$$

$$f_U = \frac{e^{-(\Delta G^\circ_{NU} + m_{NU}[D])/RT}}{1 + e^{-(\Delta G^\circ_{NU} + m_{NU}[D])/RT}} \quad (3)$$

Molecular Dynamics. In recent years, atomistically detailed molecular dynamics simulations have been widely used to complement experiments in order to provide molecular insights into denaturant-induced protein unfolding reactions,[63−70] which are often inaccessible in the commonly used experiments due to resolution limits. The initial structure of the PI3K SH3 domain (residues 3−84) was taken from the NMR structure deposited in the Protein Data Bank (PDB ID code 1PNJ). The protein was immersed in a 80 Å × 80 Å × 80 Å box of aqueous 8 M urea solution. The final system contained ∼7900 water molecules and ∼1845 urea molecules. This system consisting of a total of ∼40 000 atoms was first energy-minimized for 10 000 steps before any production of MD. The particle-mesh Ewald (PME) method[71] was used for the long-range electrostatic interactions,[72] while the van der Waals interactions were treated with a cutoff distance of 12 Å. The CHARMM22 (c32b1 parameter set) force field was used for both protein and urea.[72,73] For water, a modified TIP3P water model[74] was used with its bond lengths constrained with SHAKE/RATTLE. This combination of force-field parameters has been extensively used by us as well as by others to study protein unfolding reactions.[16,32,70] All simulations were performed using the NAMD2[75] molecular modeling package using IBM BlueGene supercomputers with a 2 fs time step in a NPT ensemble at 1 atm. The temperature was controlled using the Langevin dynamics scheme, and the pressure was controlled using the Berendsen pressure coupling implemented in NAMD. Eight MD trajectories were run starting from the initial energy minimized configurations with initial velocities assigned from a Maxwell−Boltzmann distribution at the specified temperature. The simulations were performed for 500 ns or longer. Table 1 summarizes the conditions and length of the different trajectories. Five trajectories were performed at 300−310 K to mimic experimental conditions (runs 1−5 in Table 1). Three other trajectories were run at higher temperature to check the temperature dependence of the unfolding landscape and to accelerate folding kinetics. The total aggregate simulation time was ∼4.4 μs.

The SASA values were calculated in VMD[76] using the measure SASA module, for which a probe radius of 1.4 Å was used. A cutoff distance of 5 Å between heavy atoms was considered to define a contact between two residues. A C_α−C_α native contact was considered to have formed between residues i and j ($|i - j| > 3$) if any heavy atom of residue i is within 5 Å of any heavy atom of residue j.

■ ASSOCIATED CONTENT

Supporting Information

Additional unfolding simulation trajectories and analyses. This material is available free of charge via the Internet at http://pubs.acs.org.

■ AUTHOR INFORMATION

Author Contributions

J.B.U. and P.D. designed research, A.D. and P.D. performed research, A.D., J.B.U., and P.D. analyzed data, and A.D., J.B.U., and P.D. wrote the manuscript. All authors reviewed the manuscript.

Notes

The authors declare no competing financial interest.

■ ACKNOWLEDGMENTS

This work was funded by the IBM BlueGene Science program, by the Tata Institute of Fundamental Research, and by the Department of Science and Technology, Government of India. J.B.U. is the recipient of a JC Bose National Fellowship from the Government of India.

■ REFERENCES

(1) Poland, D. C.; Scheraga, H. A. Statistical Mechanics Of Noncovalent Bonds In Polyamino Acids .Ix. 2-State Theory of Protein Denaturation. *Biopolymers* **1965**, *3*, 401−419.

(2) Bryngelson, J. D.; Onuchic, J. N.; Socci, N. D.; Wolynes, P. G. Funnels, Pathways, and the Energy Landscape of Protein Folding: A Synthesis. *Proteins* **1995**, *21*, 167−195.

(3) Dill, K. A.; Bromberg, S.; Yue, K.; Fiebig, K. M.; Yee, D. P.; Thomas, P. D.; Chan, H. S. Principles of Protein Folding–A Perspective from Simple Exact Models. *Protein Sci.* **1995**, *4*, 561−602.

(4) Onuchic, J. N.; Luthey-Schulten, Z.; Wolynes, P. G. Theory of Protein Folding: The Energy Landscape Perspective. *Annu. Rev. Phys. Chem.* **1997**, *48*, 545−600.

(5) Go, N. Theoretical Studies of Protein Folding. *Annu. Rev. Biophys. Bioeng.* **1983**, *12*, 183−210.

(6) Takada, S. Go-Ing For The Prediction of Protein Folding Mechanisms. *Proc. Natl. Acad. Sci. U.S.A.* **1999**, *96*, 11698−11700.
(7) Leopold, P. E.; Montal, M.; Onuchic, J. N. Protein Folding Funnels: A Kinetic Approach to the Sequence-Structure Relationship. *Proc. Natl. Acad. Sci. U.S.A.* **1992**, *89*, 8721−8725.
(8) Plaxco, K. W.; Simons, K. T.; Baker, D. Contact Order, Transition State Placement and the Refolding Rates of Single Domain Proteins. *J. Mol. Biol.* **1998**, *277*, 985−994.
(9) Gillespie, B.; Plaxco, K. W. Using Protein Folding Rates to Test Protein Folding Theories. *Annu. Rev. Biochem.* **2004**, *73*, 837−859.
(10) Das, P.; Wilson, C. J.; Fossati, G.; Wittung-Stafshede, P.; Matthews, K. S.; Clementi, C. Characterization of the Folding Landscape of Monomeric Lactose Repressor: Quantitative Comparison of Theory and Experiment. *Proc. Natl. Acad. Sci. U.S.A.* **2005**, *102*, 14569−14574.
(11) Mok, Y. K.; Kay, C. M.; Kay, L. E.; Forman-Kay, J. Noe Data Demonstrating a Compact Unfolded State for an Sh3 Domain under Non-Denaturing Conditions. *J. Mol. Biol.* **1999**, *289*, 619−638.
(12) Nabuurs, S. M.; De Kort, B. J.; Westphal, A. H.; Van Mierlo, C. P. Non-Native Hydrophobic Interactions Detected in Unfolded Apoflavodoxin by Paramagnetic Relaxation Enhancement. *Eur. Biophys. J.* **2010**, *39*, 689−698.
(13) Capaldi, A. P.; Kleanthous, C.; Radford, S. E. Im7 Folding Mechanism: Misfolding on a Path to the Native State. *Nat. Struct. Biol.* **2002**, *9*, 209−216.
(14) Feng, H.; Takei, J.; Lipsitz, R.; Tjandra, N.; Bai, Y. Specific Non-Native Hydrophobic Interactions in a Hidden Folding Intermediate: Implications for Protein Folding. *Biochemistry* **2003**, *42*, 12461−1265.
(15) Neudecker, P.; Zarrine-Afsar, A.; Choy, W. Y.; Muhandiram, D. R.; Davidson, A. R.; Kay, L. E. Identification of A Collapsed Intermediate with Non-Native Long-Range Interactions on the Folding Pathway of a Pair of Fyn Sh3 Domain Mutants by Nmr Relaxation Dispersion Spectroscopy. *J. Mol. Biol.* **2006**, *363*, 958−976.
(16) Das, P.; King, J. A.; Zhou, R. Beta-Strand Interactions at the Domain Interface Critical for the Stability of Human Lens Gammad-Crystallin. *Protein Sci.* **2010**, *19*, 131−140.
(17) Das, P.; King, J. A.; Zhou, R. Aggregation of Gamma-Crystallins Associated with Human Cataracts via Domain Swapping at the C-Terminal Beta-Strands. *Proc. Natl. Acad. Sci. U.S.A.* **2011**, *108*, 10514−10519.
(18) Dasgupta, A.; Udgaonkar, J. B. Transient Non-Native Burial of a Trp Residue Occurs Initially during the Unfolding of a Sh3 Domain. *Biochemistry* **2012**, *51*, 8226−8234.
(19) Neudecker, P.; Robustelli, P.; Cavalli, A.; Walsh, P.; Lundstrom, P.; Zarrine-Afsar, A.; Sharpe, S.; Vendruscolo, M.; Kay, L. E. Structure of an Intermediate StateiIn Protein Folding and Aggregation. *Science* **2012**, *336*, 362−366.
(20) Clementi, C.; Plotkin, S. S. The Effects of Nonnative Interactions on Protein Folding Rates: Theory and Simulation. *Protein Sci.* **2004**, *13*, 1750−1766.
(21) Das, P.; Matysiak, S.; Clementi, C. Balancing Energy And Entropy: A Minimalist Model for the Characterization of Protein Folding Landscapes. *Proc. Natl. Acad. Sci. U.S.A.* **2005**, *102*, 10141−10146.
(22) Faisca, P. F.; Nunes, A.; Travasso, R. D.; Shakhnovich, E. I. Non-Native Interactions Play an Effective Role in Protein Folding Dynamics. *Protein Sci.* **2010**, *19*, 2196−2209.
(23) Li, L.; Mirny, L. A.; Shakhnovich, E. I. Kinetics, Thermodynamics and Evolution of Non-Native Interactions in a Protein Folding Nucleus. *Nat. Struct. Biol.* **2000**, *7*, 336−342.
(24) Zarrine-Afsar, A.; Wallin, S.; Neculai, A. M.; Neudecker, P.; Howell, P. L.; Davidson, A. R.; Chan, H. S. Theoretical and Experimental Demonstration of the Importance of Specific Nonnative Interactions in Protein Folding. *Proc. Natl. Acad. Sci. U.S.A.* **2008**, *105*, 9999−10004.
(25) Ferreiro, D. U.; Hegler, J. A.; Komives, E. A.; Wolynes, P. G. On the Role of Frustration in the Energy Landscapes of Allosteric Proteins. *Proc. Natl. Acad. Sci. U.S.A.* **2011**, *108*, 3499−3503.
(26) Wani, A. H.; Udgaonkar, J. B. Revealing a Concealed Intermediate that forms after the Rate-Limiting Step of Refolding of the Sh3 Domain of Pi3 Kinase. *J. Mol. Biol.* **2009**, *387*, 348−362.
(27) Wani, A. H.; Udgaonkar, J. B. Native State Dynamics Drive The Unfolding of the Sh3 Domain of Pi3 Kinase at High Denaturant Concentration. *Proc. Natl. Acad. Sci. U.S.A.* **2009**, *106*, 20711−20716.
(28) Dasgupta, A.; Udgaonkar, J. B. Evidence for Initial Non-Specific Polypeptide Chain Collapse during the Refolding of the Sh3 Domain of Pi3 Kinase. *J. Mol. Biol.* **2010**, *403*, 430−445.
(29) Dasgupta, A.; Udgaonkar, J. B. Four-State Folding Of A Sh3 Domain: Salt-Induced Modulation of the Stabilities of the Intermediates and Native State. *Biochemistry* **2012**, *51*, 4723−4734.
(30) Finkelstein, A. V.; Shakhnovich, E. I. Theory of Cooperative Transitions in Protein Molecules. Ii. Phase Diagram for a Protein Molecule in Solution. *Biopolymers* **1989**, *28*, 1681−1694.
(31) Baldwin, R. L.; Frieden, C.; Rose, G. D. Dry Molten Globule Intermediates and the Mechanism of Protein Unfolding. *Proteins* **2010**, *78*, 2725−2737.
(32) Hua, L.; Zhou, R.; Thirumalai, D.; Berne, B. J. Urea Denaturation by Stronger Dispersion Interactions with Proteins than Water Implies a 2-Stage Unfolding. *Proc. Natl. Acad. Sci. U.S.A.* **2008**, *105*, 16928−16933.
(33) Gao, M.; She, Z. S.; Zhou, R. Key Residues that play a Critical Role in Urea-Induced Lysozyme Unfolding. *J. Phys. Chem. B* **2010**, *114*, 15687−15693.
(34) Bennion, B. J.; Daggett, V. The Molecular Basis for the Chemical Denaturation of Proteins by Urea. *Proc. Natl. Acad. Sci. U.S.A.* **2003**, *100*, 5142−5147.
(35) Lim, W. K.; Rosgen, J.; Englander, S. W. Urea, but not Guanidinium, Destabilizes Proteins by forming Hydrogen Bonds to the Peptide Group. *Proc. Natl. Acad. Sci. U.S.A.* **2009**, *106*, 2595−2600.
(36) Sridevi, K.; Udgaonkar, J. B. Surface Expansion is Independent of and Occurs Faster than Core Solvation during the Unfolding of Barstar. *Biochemistry* **2003**, *42*, 1551−1563.
(37) Lakshmikanth, G. S.; Sridevi, K.; Krishnamoorthy, G.; Udgaonkar, J. B. Structure is Lost Incrementally during the Unfolding of Barstar. *Nat. Struct. Biol.* **2001**, *8*, 799−804.
(38) Jha, S. K.; Dhar, D.; Krishnamoorthy, G.; Udgaonkar, J. B. Continuous Dissolution of Structure during the Unfolding of a Small Protein. *Proc. Natl. Acad. Sci. U.S.A.* **2009**, *106*, 11113−11118.
(39) Heinig, M.; Frishman, D. Stride: A Web Server for Secondary Structure Assignment from Known Atomic Coordinates of Proteins. *Nucleic Acids Res.* **2004**, *32* (WebServer Issue), W500-2.
(40) Chan, H. S.; Bromberg, S.; Dill, K. A. Models of Cooperativity in Protein Folding. *Philos. Trans. R. Soc. London, Ser. B* **1995**, *348*, 61−70.
(41) Parker, M. J.; Marqusee, S. The Cooperativity of Burst Phase Reactions Explored. *J. Mol. Biol.* **1999**, *293*, 1195−1210.
(42) Sinha, K. K.; Udgaonkar, J. B. Dependence of the Size of The Initially Collapsed Form during the Refolding ff Barstar on Denaturant Concentration: Evidence for a Continuous Transition. *J. Mol. Biol.* **2005**, *353*, 704−718.
(43) Sinha, K. K.; Udgaonkar, J. B. Barrierless Evolution of Structure during the Submillisecond Refolding Reaction of a Small Protein. *Proc. Natl. Acad. Sci. U.S.A.* **2008**, *105*, 7998−8003.
(44) Dasgupta, A.; Udgaonkar, J. B. Evidence for Initial Non-Specific Polypeptide Chain Collapse during the Refolding of The Sh3 Domain of Pi3 Kinase. *J. Mol. Biol.* **2010**, *403*, 430−445.
(45) Selvaraj, S.; Gromiha, M. M. Role Of Hydrophobic Clusters and Long-Range Contact Networks in The Folding Of (Alpha/Beta)8 Barrel Proteins. *Biophys. J.* **2003**, *84*, 1919−1925.
(46) Meng, W.; Lyle, N.; Luan, B.; Raleigh, D. P.; Pappu, R. V. Experiments And Simulations Show How Long-Range Contacts Can Form in Expanded Unfolded Proteins with Negligible Secondary Structure. *Proc. Natl. Acad. Sci. U.S.A.* **2013**, *110*, 2123−2128.
(47) Goldenberg, D. P. Computational Simulation Of The Statistical Properties of Unfolded Proteins. *J. Mol. Biol.* **2003**, *326*, 1615−1633.

(48) Ahmad, A.; Millett, I. S.; Doniach, S.; Uversky, V. N.; Fink, A. L. Stimulation of Insulin Fibrillation by Urea-Induced Intermediates. *J. Biol. Chem.* **2004**, *279*, 14999−15013.
(49) Schwalbe, H.; Fiebig, K. M.; Buck, M.; Jones, J. A.; Grimshaw, S. B.; Spencer, A.; Glaser, S. J.; Smith, L. J.; Dobson, C. M. Structural And Dynamical Properties Of A Denatured Protein. Heteronuclear 3D Nmr Experiments and Theoretical Simulations of Lysozyme in 8 M Urea. *Biochemistry* **1997**, *36*, 8977−8991.
(50) Mok, Y. K.; Kay, C. M.; Kay, L. E.; Forman-Kay, J. Noe Data Demonstrating a Compact Unfolded State for an Sh3 Domain under Non-Denaturing Conditions. *J. Mol. Biol.* **1999**, *289*, 619−638.
(51) Neri, D.; Billeter, M.; Wider, G.; Wuthrich, K. Nmr Determination of Residual Structure in a Urea-Denatured Protein, The 434-Repressor. *Science* **1992**, *257*, 1559−1563.
(52) Ackerman, M. S.; Shortle, D. Robustness Of The Long-Range Structure in Denatured Staphylococcal Nuclease to Changes in Amino Acid Sequence. *Biochemistry* **2002**, *41*, 13791−13797.
(53) Klein-Seetharaman, J.; Oikawa, M.; Grimshaw, S. B.; Wirmer, J.; Duchardt, E.; Ueda, T.; Imoto, T.; Smith, L. J.; Dobson, C. M.; Schwalbe, H. Long-Range Interactions within a Nonnative Protein. *Science* **2002**, *295*, 1719−1722.
(54) Prieto, J.; Wilmans, M.; Jimenez, M. A.; Rico, M.; Serrano, L. Non-Native Local Interactions in Protein Folding and Stability: Introducing a Helical Tendency in the All Beta-Sheet Alpha-Spectrin Sh3 Domain. *J. Mol. Biol.* **1997**, *268*, 760−778.
(55) Gorovits, B. M.; Seale, J. W.; Horowitz, P. M. Residual Structure in Urea-Denatured Chaperonin Groel. *Biochemistry* **1995**, *34*, 13928−13933.
(56) Hodsdon, M. E.; Frieden, C. Intestinal Fatty Acid Binding Protein: The Folding Mechanism as Determined By Nmr Studies. *Biochemistry* **2001**, *40*, 732−742.
(57) Li, J.; Shinjo, M.; Matsumura, Y.; Morita, M.; Baker, D.; Ikeguchi, M.; Kihara, H. An Alpha-Helical Burst in the Src Sh3 Folding Pathway. *Biochemistry* **2007**, *46*, 5072−5082.
(58) Matsumura, Y.; Shinjo, M.; Kim, S. J.; Okishio, N.; Gruebele, M.; Kihara, H. Transient Helical Structure During Pi3k and Fyn Sh3 Domain Folding. *J. Phys. Chem. B* **2013**, *117*, 4836−4843.
(59) Xiu, P.; Yang, Z.; Zhou, B.; Das, P.; Fang, H.; Zhou, R. Urea-Induced Drying of Hydrophobic Nanotubes: Comparison of Different Urea Models. *J. Phys. Chem. B* **2011**, *115*, 2988−2994.
(60) Canchi, D. R.; Paschek, D.; Garcia, A. E. Equilibrium Study of Protein Denaturation By Urea. *J. Am. Chem. Soc.* **2010**, *132*, 2338−2344.
(61) Candotti, M.; Esteban-Martãn, S.; Salvatella, X.; Orozco, M. Toward an Atomistic Description of the Urea-Denatured State of Proteins. *Proc. Natl. Acad. Sci. U.S.A.* **2013**, *110*, 5933−5938.
(62) Bader, R.; Bamford, R.; Zurdo, J.; Luisi, B. F.; Dobson, C. M. Probing The Mechanism Of Amyloidogenesis Through A Tandem Repeat of the Pi3-Sh3 Domain Suggests a Generic Model for Protein Aggregation and Fibril Formation. *J. Mol. Biol.* **2006**, *356*, 189−208.
(63) Bennion, B. J.; Daggett, V. The Molecular Basis for the Chemical Denaturation of Proteins by Urea. *Proc. Natl. Acad. Sci. U.S.A.* **2003**, *100*, 5142−5147.
(64) Camilloni, C.; Rocco, A. G.; Eberini, I.; Gianazza, E.; Broglia, R. A.; Tiana, G. Urea and Guanidinium Chloride Denature Protein L in Different Ways in Molecular Dynamics Simulations. *Biophys. J.* **2008**, *94*, 4654−4661.
(65) Das, P.; Xia, Z.; Zhou, R. Collapse of A Hydrophobic Polymer in A Mixture of Denaturants. *Langmuir* **2013**, *29*, 4877−4882.
(66) Godawat, R.; Jamadagni, S. N.; Garde, S. Unfolding of Hydrophobic Polymers in Guanidinium Chloride Solutions. *J. Phys. Chem. B* **2010**, *114*, 2246−2254.
(67) O'brien, E. P.; Dima, R. I.; Brooks, B.; Thirumalai, D. Interactions between Hydrophobic and Ionic Solutes in Aqueous Guanidinium Chloride and Urea Solutions: Lessons for Protein Denaturation Mechanism. *J. Am. Chem. Soc.* **2007**, *129*, 7346−7353.
(68) Tran, H. T.; Mao, A.; Pappu, R. V. Role of Backbone-Solvent Interactions in Determining Conformational Equilibria of Intrinsically Disordered Proteins. *J. Am. Chem. Soc.* **2008**, *130*, 7380−7392.
(69) Wallqvist, A.; Smythers, G. W.; Covell, D. G. A Cooperative Folding Unit In Hiv-1 Protease. Implications For Protein Stability And Occurrence Of Drug-Induced Mutations. *Protein Eng.* **1998**, *11*, 999−1005.
(70) Xia, Z.; Das, P.; Shakhnovich, E. I.; Zhou, R. Collapse af Unfolded Proteins in a Mixture of Denaturants. *J. Am. Chem. Soc.* **2012**, *134*, 18266−18274.
(71) Deserno, M.; Holm, C. How To Mesh Up Ewald Sums. I. A Theoretical and Numerical Comparison of Various Particle Mesh Routines. *J. Chem. Phys.* **1998**, *109*, 7678.
(72) Brooks, B. R.; Brooks, C. L., 3rd; Mackerell, A. D., Jr.; Nilsson, L.; Petrella, R. J.; Roux, B.; Won, Y.; Archontis, G.; Bartels, C.; Boresch, S.; et al. The Biomolecular Simulation Program. *J. Comput. Chem.* **2009**, *30*, 1545−1614.
(73) Mackerell, A. D.; Bashford, D.; Bellott, M.; Evanseck, J. D.; J., R. L. D.; Field, M. J.; Fischer, S.; Gao, J.; Guo, H.; Ha, S.; Joseph, D.; et al. All-Atom Empirical Potential for Molecular Modeling fnd Dynamics Studies of Proteins. *J. Phys. Chem. B* **1998**, *102*, 3586−3616.
(74) Jorgensen, W. L.; Chandrasekhar, J.; Madura, J. D.; Impey, R. W.; Klein, M. L. Comparison of Simple Potential Functions for Simulating Liquid Water. *J. Chem. Phys.* **1983**, *79*, 926.
(75) Kumar, S.; Huang, C.; Zheng, G.; Bohm, E.; Bhatele, A.; Phillips, J. C.; Yu, H.; Kale, L. V. Scalable Molecular Dynamics with Namd on the Ibm Blue Gene/L System. *IBM J. Res. Dev.* **2008**, *52* (1/2), 177−178.
(76) Humphrey, W.; Dalke, A.; Schulten, K. Vmd: Visual Molecular Dynamics. *J. Mol. Graphics* **1996**, *14* (33−8), 27−28.
(77) Pettersen, E. F.; Goddard, T. D.; Huang, C. C.; Couch, G. S.; Greenblatt, D. M.; Meng, E. C.; Ferrin, T. E. Ucsf Chimera–A Visualization System for Exploratory Research and Analysis. *J. Comput. Chem.* **2004**, *25*, 1605−1612.